CHEMISTRY
A EUROPEAN JOURNAL

DOI: 10.1002/chem.200902861

Three-Dimensional Antiferromagnetic Order of Single-Chain Magnets: A New Approach to Design Molecule-Based Magnets

Hitoshi Miyasaka,*[a] Karin Takayama,[a] Ayumi Saitoh,[d] Sachie Furukawa,[d] Masahiro Yamashita,[a] and Rodolphe Clérac*[b, c]

Dedicated to the memory of Dr. Ian Hewitt

Abstract: Two one-dimensional compounds composed of a 1:1 ratio of Mn^{III} salen-type complex and Ni^{II} oximato moiety with different counter anions, PF_6^- and BPh_4^-, were synthesized: $[Mn(3,5\text{-}Cl_2saltmen)Ni(pao)_2(phen)]PF_6$ (**1**) and $[Mn(5\text{-}Clsaltmen)Ni(pao)_2(phen)]BPh_4$ (**2**), where $3,5\text{-}Cl_2saltmen^{2-}$ = *N*,*N*′-(1,1,2,2-tetramethylethylene)bis(3,5-dichlorosalicylideneiminate); $5\text{-}Clsaltmen^{2-}$ = *N*,*N*′-(1,1,2,2-tetramethylethylene)-bis(5-chlorosalicylideneiminate); pao^- = pyridine-2-aldoximate; and phen = 1,10-phenanthroline. Single-crystal X-ray diffraction study was carried out for both compounds. In **1** and **2**, the chain topology is very similar forming an alternating linear chain with a [-Mn^{III}-ON-Ni^{II}-NO-] repeating motif (where -ON- is the oximate bridge). The use of a bulky counteranion, such as BPh_4^-, located between the chains in **2** rather than PF_6^- in **1**, successfully led to the magnetic isolation of the chains in **2**. This minimization of the interchain interactions allows the study of the intrinsic magnetic properties of the chains present in **1** and **2**. While **1** and **2** possess, as expected, very similar paramagnetic properties above 15 K, their ground state is antiferromagnetic below 9.4 K and paramagnetic down to 1.8 K, respectively. Nevertheless, both compounds exhibit a magnet-type behavior at temperatures below 6 K. While for **2**, the observed magnetism is well explained by a Single-Chain Magnet (SCM) behavior, the magnet properties for **1** are induced by the presence in the material of SCM building units that order antiferromagnetically. By controlling both intra- and interchain magnetic interactions in this new [$Mn^{III}Ni^{II}$] SCM system, a remarkable AF phase with a magnet-type behavior has been stabilized in relation with the intrinsic SCM properties of the chains present in **1**. This result suggests that the simultaneous enhancement of both intrachain (J) and interchain (J') magnetic interactions (with keeping $J \gg J'$), independently of the presence of AF phase might be an efficient route to design high temperature SCM-based magnets.

Keywords: antiferromagnetism · coordination chemistry · low dimensionality · magnetic properties · single-chain magnets

Introduction

Since the discovery of magnet-type behavior in isolated molecules, called Single-Molecule Magnets (SMMs),[1] in the beginning of 1990s and in one-dimensional (1D) systems, called Single-Chain Magnets (SCMs),[2] in 2001,[3] all scientists who targeted to prepare these superparamagnetic-like systems have tried to isolate them using different synthetic

[a] Prof. H. Miyasaka, K. Takayama, Prof. M. Yamashita
Department of Chemistry, Graduate School of Science
Tohoku University, 6-3 Aramaki-Aza-Aoba
Aoba-ku, Sendai, Miyagi 980-8578 (Japan)
Fax: (+81) 22-795-6548
E-mail: miyasaka@agnus.chem.tohoku.ac.jp

[b] Dr. R. Clérac
CNRS, UPR 8641, Centre de Recherche Paul Pascal (CRPP)
Equipe "Matériaux Moléculaires Magnétiques"
115 avenue du Dr. Albert Schweitzer, 33600 Pessac (France)
Fax: (+33) 556-84-5600
E-mail: clerac@crpp-bordeaux.cnrs.fr

[c] Dr. R. Clérac
Université de Bordeaux, UPR 8641, 33600 Pessac (France)

[d] A. Saitoh, S. Furukawa
Department of Chemistry, Graduate School of Science
Tokyo Metropolitan University, 1-1 Minami-ohsawa
Hachioji, Tokyo 192-0397 (Japan)

Supporting information for this article is available on the WWW under http://dx.doi.org/10.1002/chem.200902861.

tools. The goal of such strategies was to avoid inter-SMM or -SCM magnetic interactions responsible for the stabilization of a three-dimensional (3D) magnetic order that was believed to prevent the intrinsic slow dynamics of the magnetization in these SMM or SCM systems. Recently, the discovery of a magnet-type behavior in antiferromagnetic (AF) and ferromagnetic (F) ordered phases of SCMs has marked the end of this dogma. Coulon et al. demonstrated experimentally and theoretically that antiferromagnetic interactions between SCMs stabilize, as planned, a 3D antiferromagnetic order without preventing the slow relaxation of the magnetization induced by the SCM components of the material.[4] Moreover, the relaxation time of this type of system, already large in zero field, is even enhanced under a DC field and maximum close to the AF-paramagnetic (P) transition line. On the other hand, Ishida and co-workers have reported the observation of slow relaxation of the magnetization in an ordered ferrimagnetic phase for a compound based on Co^{II}–radical chains[5] similar to the SCM system reported by Caneschi at al.[3] Even if slow dynamics is often observed in ferromagnetic or ferrimagnetic ordered systems, Sessoli suggested that the unusually large coercive field (52 kOe) in Ishida's material might be related to the intrinsic slow dynamics of the chains present in this compound.[6] These two types of systems and magnetic ground states are very different but it seems quite general that an ordered magnetic phase, even of antiferromagnetic nature, can display slow dynamics of its magnetization induced by the presence of SCM units in the material. These astonishing results inspired us to design a new type of magnets based on SCMs controlling intrinsic SCM parameters and enhancing the interchain magnetic interactions.

In the past ten years, our group has developed a broad knowledge on the chemistry of Mn^{III} salen-type complexes and their assemblies[7] in particular with oximate-based[8,9] and cyano-based[10] complexes. Among the reported materials, the family of $[Mn_2(saltmen)_2Ni(pao)_2(L)_n](A)_2$ (saltmen^{2-} = *N*,*N*′-(1,1,2,2-tetramethylethylene)bis(salicylideneiminate) and pao$^-$ = pyridine-2-aldoximate, L = mono- or bidentate ligands with $n = 2$ and 1, respectively, and A = monoanion),[2a,11] is probably the most interesting system. The simplicity of the chain topology and the amplitude of the intrinsic magnetic parameters made them unique textbook examples for the SCM behavior,[2b,12] allowing us to achieve an unprecedented deep understanding of this property.[13] Recently, the functionalization of the saltmen ligand on the 5-position by a methoxy group resulted in increasing the interchain interactions (without changing the structural and magnetic topology of the chain) in $[Mn_2(5\text{-MeOsaltmen})_2Ni(pao)_2(phen)](PF_6)_2$ (phen = 1,10-phenanthroline, 5-MeOsaltmen^{2-} = *N*,*N*′-(1,1,2,2-tetramethylethylene)bis(5-methoxysalicylideneiminate)).[4] However, until the present work, we have been unable i) to increase the intrachain interactions that are directly associated with the magnetization dynamics and ii) to control in the same time the interchain coupling. Herein, we report two new materials that illustrate this dual achievement and a new synthetic approach to design new molecule-based magnets using an AF phase of SCMs.

Results and Discussion

The reaction of $[Mn^{III}(3,5\text{-}Cl_2saltmen)(H_2O)(MeOH)]PF_6$ (where 3,5-Cl$_2$saltmen^{2-} = *N*,*N*′-(1,1,2,2-tetramethylethylene)bis(3,5-dichlorosalicylideneiminate)) with $[Ni^{II}(pao)_2(phen)]$ in a mixing ratio of 1:1 in a methanol/CH_2Cl_2 medium yielded $[Mn(3,5\text{-}Cl_2saltmen)Ni(pao)_2(phen)]PF_6$ (**1**) (see Experimental Section). Gold-brown crystals suitable for single-crystal X-ray crystallographic analysis (see below) are obtained within a few hours in high yield. Nevertheless, it is worth mentioning that the slow diffusion technique described in the Experimental Section is better than the bulk synthesis method to prepare relatively large single crystals of **1** (note that a di-μ-oxo Mn^{IV} dinuclear complex, $[\{Mn^{IV}(3,5\text{-}Cl_2saltmen)\}_2(\mu\text{-}O)_2]$ is often co-crystallizing in this method, therefore the crystalline material should be systematically checked by X-ray diffraction before measuring the magnetic properties).

In order to determine the intrinsic magnetic properties of the chain present in **1**, a reference compound has been designed using a bulky counter ion, BPh_4^-, to minimize the interchain magnetic interactions owing to a significant separation of the chains. Indeed, the same synthetic strategy has already been successfully employed in the original $Mn^{III}_2Ni^{II}$ SCM family with the synthesis of $[Mn_2(saltmen)_2Ni(pao)_2(phen)](BPh_4)_2$ that exhibits "perfect" or textbook SCM properties.[11c] In this vein, $[Mn(5\text{-}Clsaltmen)Ni(pao)_2(phen)]BPh_4$ (**2**) has been synthesized by a 1:2 (or 1:1 Mn/Ni ratio) reaction of $[Mn_2(5\text{-}Clsaltmen)_2(H_2O)_2](ClO_4)_2$ and $[Ni(pao)_2(phen)]$ in the presence of four equivalents of BPh_4^- (where 5-Clsaltmen^{2-} = *N*,*N*′-(1,1,2,2-tetramethylethylene)bis(5-chlorosalicylideneiminate)). Note that by tuning synthetic conditions (solvent, stoichiometry, crystallization method, etc), substitutions on saltmen and L ligand used, we have thus been able to obtain unprecedented 1:1 ($Mn^{III}Ni^{II}$) chains in the associative chemistry of Mn^{III} salen-type units and oximate-based complexes.

Single-crystal X-ray crystallography was carried out for **1** and **2** (Figure 1) and the structural parameters are summarized in the Experimental Section. As expected, the chain topology of these two compounds is very similar, forming an alternating linear chain with a [-Mn^{III}-ON-Ni^{II}-NO-] repeating motif (where -ON- is the oximate bridge) as depicted in Figure 1. It is worth mentioning that in the $[Mn_2(saltmen)_2Ni(pao)_2(L)_n](A)_2$ series, the chain topology consisted of a [Mn^{III}-$(O)_2$-Mn^{III}-ON-Ni^{II}-NO-] repeating motif, in which the SCM behavior was governed by a weak intrachain Mn^{III}–Mn^{III} ferromagnetic coupling of about +0.4 to +0.9 K through the -$(O)_2$- bi-phenolate bridge.[2,11] In contrast, the Mn^{III}–Ni^{II} intrachain magnetic interaction through the oximate bridge in **1** and **2** is known to mediate relatively strong antiferromagnetic interaction of about −20 K.[2,11] In both compounds, the Mn ion has an elongated octahedral

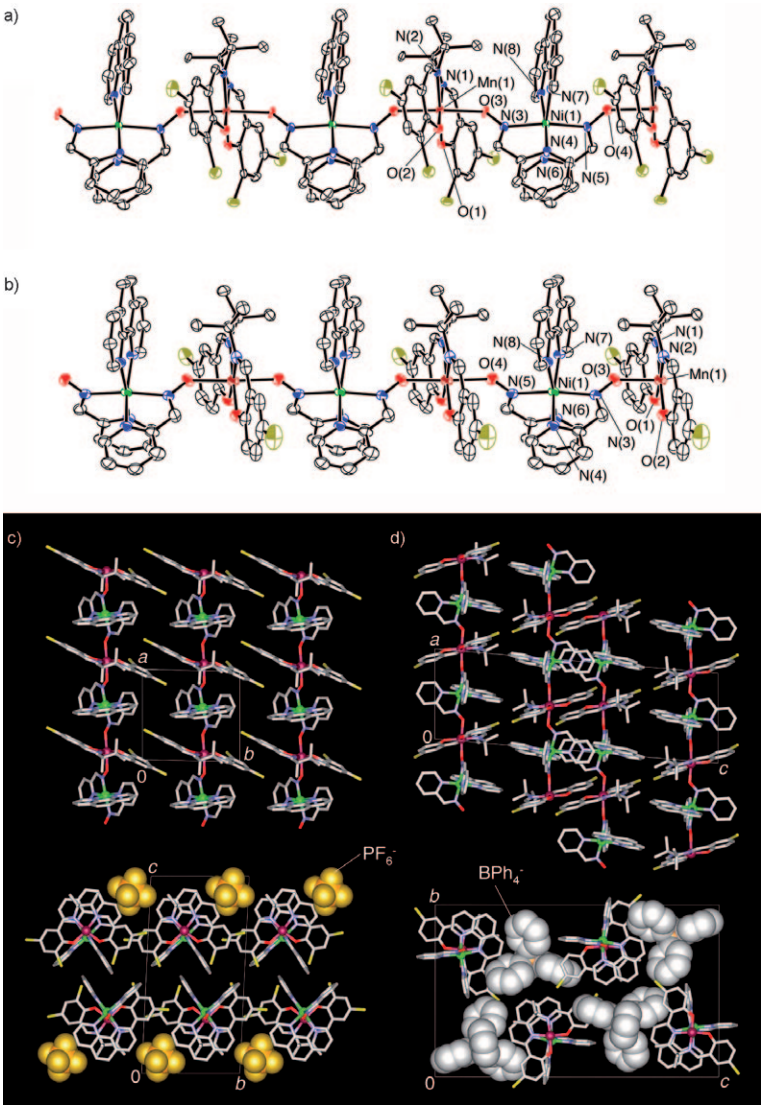

Figure 1. ORTEP type views of the one-dimensional chain motifs in **1** (a) and **2** (b) with 50% probability thermal ellipsoids. Packing diagrams of **1** (c) and **2** (d): the top and bottom figures are side and top views on chains, respectively. The side view for **1** (top of c) displays only one chain-layer. Hydrogen atoms, solvents molecules occupying void space, and counter anions for side views are omitted for clarity. Bond lengths [Å] and angles [°] for **1**: Mn(1)–$O(3)_{oxime}$ 2.183(4), Mn(1)–$O(4)_{oxime}$ 2.243(4), Ni(1)–$N(3)_{oxime}$ 2.057(5), Ni(1)–$N(5)_{oxime}$ 2.083(5); Mn(1)-O(3)-N(3) 134.6(3), Mn(1)-O(4)-N(5) 135.2(4), Ni(1)-N(3)-O(3) 122.6(3), Ni(1)-N(5)-O(4) 125.8(4); for **2**: Mn(1)–$O(3)_{oxime}$ 2.167(3), Mn(1)–$O(4)_{oxime}$ 2.154(3), Ni(1)–$N(3)_{oxime}$ 2.040(3), Ni(1)–$N(5)_{oxime}$ 2.047(3); Mn(1)-O(3)-N(3) 135.3(2), Mn(1)-O(4)-N(5) 132.9(2), Ni(1)-N(3)-O(3) 23.5(2), Ni(1)-N(5)-O(4) 123.3(2).

geometry, in which the elongated axis, corresponding to the Jahn–Teller direction, is located along the out-of-plane Mn–O_{oxime} bond. The equatorial bond lengths are found in the range of 1.91–1.95 Å for Mn–O_{Ph} and 2.00–2.02 Å for Mn–N_{imine}. The Ni moiety has an NO-*trans* geometry and exists in both Δ and Λ isomeric forms in the structure.[9] A given chain is composed of only one type of isomeric conformations but Δ and Λ chains are alternately found in the crystal structures leading to racemic packings (see below). The distorted octahedral geometry of the Ni^{II} ion is indeed with similar in terms of bond lengths and angles to what is observed in the precursors.[9] Overall, the chain structure in both materials possesses very similar bond lengths and angles (legend of Figure 1) in such a way that these chains in **1** and **2** should display the same intrinsic magnetic properties.

It is important to compare the packing arrangement of the chains in **1** and **2** (Figure 1c and d), as the interchain magnetic interactions will be a critical parameter in the following discussion of the magnetic properties. While chains (Δ and Λ chains are noted C_Δ and C_Λ, respectively) and PF_6^- counteranions form segregated layers parallel to the *ab* plane with a $[\cdots C_\Delta \cdots C_\Lambda \cdots PF_6 \cdots C_\Delta \cdots C_\Lambda \cdots PF_6 \cdots]$ stacking mode along the *c* axis in **1** (Figure 1c), the packing arrangement of **2** is completely different with large BPh_4^- anions that, as planned, evenly separate Δ and Λ chains (Figure 1d). Even if the shortest interchain distances between magnetic centers are relatively large in both compounds (Ni···Ni = 9.22 Å and Mn···Mn = 10.56 Å in **1** and Ni···Ni = 10.04 Å and Mn···Mn = 11.10 Å in **2**), interchain π–π contacts between saltmen phenyl rings are found only in **1** along the *b* axis (with C···C = 3.33 Å, see Figure S1, Supporting Information), which could be at the origin of the different magnetic properties observed for **1** and **2** (see below).

DC magnetic susceptibilities of **1** and **2** were measured on polycrystalline samples between 1.8 to 300 K at 0.1 T (Figure 2 and S2). As expected based on the crystallographic analysis, the two compounds have almost identical χT vs T behaviors. The χT product decreases when the temperature is lowered from 300 to about 50 K revealing the presence of intrachain Mn^{III}–Ni^{II} antiferromagnetic interactions as already observed in related systems.[2,11] Lowering temperature, the χT product increases as expected for ferrimagnetically-arranged systems and finally decreases below 9 K. To model the static magnetic properties of these compounds, an alternating Heisenberg chain model of classical spins (with $H = -2J\sum_{i=1}^{N}(S_i \cdot s_i + s_i \cdot S_{i+1})$ and $S_i = S_{Mn} = 2$ and $s_i = S_{Ni} = 1$),

was employed. The expression of the susceptibility given by Georges et al.[14] was used to fit the data between 20–300 K (solid lines in Figure 2 and S2) with the following best set of parameters: $g_{Mn}=2.00(5)$, $g_{Ni}=2.13(5)$, $J/k_B=-21.5(2)$ K for **1** and $g_{Mn}=1.95(5)$, $g_{Ni}=1.99(5)$, $J/k_B=-21.1(2)$ K for **2**. It is worth noting that the value of $J/k_B \approx -21$ K is commonly found for Mn^{III}–Ni^{II} magnetic interaction through the oximate bridge and consistent with related systems.[2,8,11]

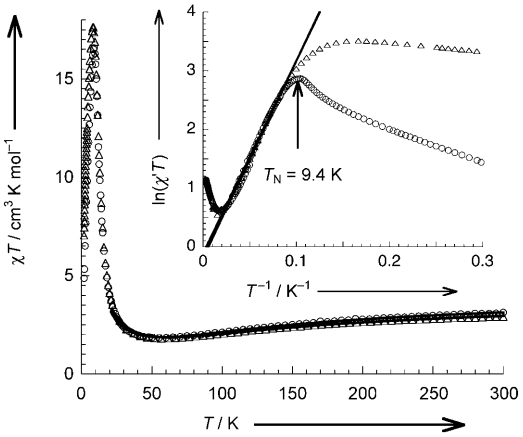

Figure 2. Temperature dependence of χT product (χ being the molar magnetic susceptibility defined as M/H per [MnNi] unit) for **1** (○) and **2** (△) under 0.1 T. The solid lines represent the best fit using an alternating chain model of isotropic classical spins. Inset: $\ln(\chi' T)$ vs $1/T$ plot (χ' being the in-phase ac magnetic susceptibility in zero DC field, in a 3 Oe AC field and with an AC frequency of 1 Hz). The solid lines are the best fits obtained using a one-dimensional Ising model.

The one-dimensional behavior of these compounds can also be checked following the correlation length, ξ, that is proportional to the χT product at zero DC field in any 1D classical problem. As shown in the inset of Figure 2, the $\ln(\chi' T)$ vs T^{-1} plot is linear between 40 and 11 K supporting an anisotropic Heisenberg or Ising-like 1D behavior.[15,16] Nakamura et al. demonstrated that the corresponding gap, $\Delta_\xi/k_B=33.6$ K for both compounds, is directly the energy to create a domain wall in the chain.[16,17] In the Ising limit, this gap should be equal to $\Delta_\xi=4JS_1S_2$ for ferrimagnetic-type chains.[2b,18] Based on the above estimation of J, $4JS_1S_2$ is about equal to 168 K which proves that these systems are not in the Ising limit and possess broad domain walls induced by large intrachain interactions. In the present limit, an analytical expression of Δ_ξ is still unknown. Nevertheless, a significant magnetic anisotropy is seen on the field dependences of the magnetization (M) at 1.8 K that are linear at high fields without saturation even at 7 T (Figure S3). The extrapolation of the magnetization at the expected saturation value is respectively 16 and 18 T for **1** and **2** that correspond to a energy of anisotropy, K_A,[19] of about 10 and 11.5 K. The fact that Δ_ξ and K_A are almost identical in **1** and **2** proves that the chains composing these materials possess the same intrinsic magnetic properties. Below 10 K ($T^{-1}=0.1$ K^{-1}), the $\ln(\chi' T)$ vs T^{-1} curve saturates for **2** as expected in the finite-size regime of SCM,[2,13] while it drops significantly at about 9 K in the case of **1**. This peculiar behavior is indeed related to the M vs H data (Figure S4) that exhibits a typical S-shape curve below 9 K (also seen as a maximum on the dM/dH vs H plot, Figure S5) indicating the presence of a field-induced phenomenon absent in **2**. Combined M vs H (Figures S4 and S5) and χ vs T (Figure S6) data allowed us to follow this characteristic field, H_C, in the (T, H) phase diagram. As shown in Figure 3, H_C is about

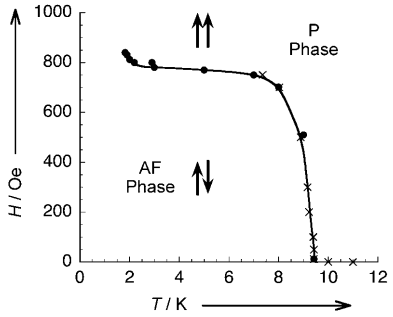

Figure 3. (T,H) phase diagram for **1**. ●: Location of the maximum of susceptibility from dM/dH vs H data (Figure S5); ×: Location of the maximum of susceptibility from χ vs T data (Figure S6); the solid line is a guide.

800 Oe at 2 K and decreases continuously to vanish at 9.4 K. The line described by $H_C(T)$ is typical of a P–AF transition line in metamagnetic materials. Hence, **1** possesses an ordered antiferromagnetic ground state below $T_N=9.4$ K, while **2** displays paramagnetic properties down to 1.8 K.

Quite surprisingly considering the difference of ground state for **1** and **2**, both compounds exhibit a magnet-type behavior, as shown in Figure 4 by large hysteresis loops ob-

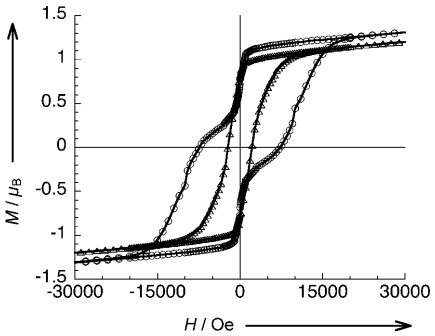

Figure 4. Field dependence of the magnetization for **1** (○) and **2** (▲) at 1.8 K measured with an average sweep-rate of about 150 Oe min^{-1}. Solid lines are guides.

served at 1.8 K (coercive fields are 7 and 2 kOe for **1** and **2**, respectively). Therefore the magnetic dynamics of these systems has been studied using ac susceptibility measurements below 15 K (Figure 5, 6, S7, S8 and S9). Below 6 K, both components of the ac susceptibility of **1** and **2** become frequency dependent as observed in related SCMs.[2,11] From

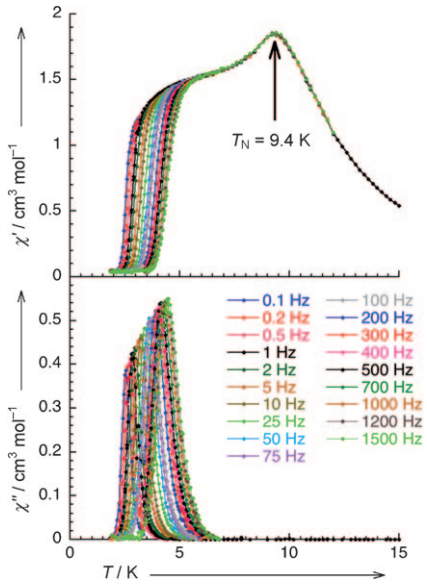

Figure 5. Temperature dependence of the real (χ') and imaginary (χ'') parts of the ac susceptibility for **1** in zero dc-field at different ac frequency and with a 3 Oe ac field. Solid lines are guides.

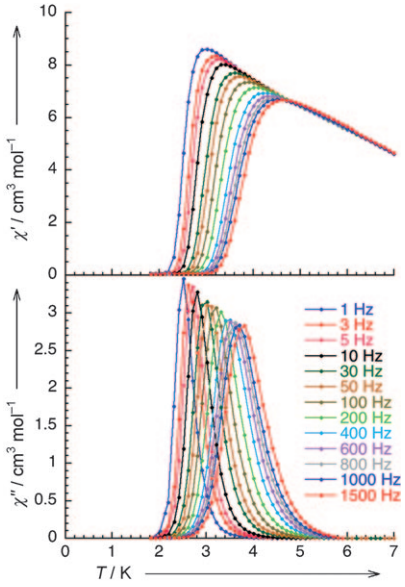

Figure 6. Temperature dependence of the real (χ') and imaginary (χ'') parts of the AC susceptibility for **2** in zero dc-field at different ac frequency and with a 3 Oe ac field. Solid lines are guides.

these data, the characteristic times have been estimated and fit to Arrhenius laws (Figure 7). The corresponding energy gaps, Δ_τ, are 55 and 54 K and the pre-exponential factors, τ_0, are about 3.9×10^{-10} and 0.7×10^{-10} s for **1** and **2**, respectively. Obviously, the presence of an antiferromagnetic order in **1** at 9.4 K does not preclude the slow dynamics with a relaxation time similar to the one measured for **2** that exhibit "pristine" SCM properties. With Δ_τ mostly unchanged and

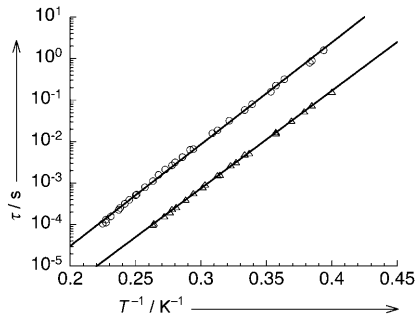

Figure 7. Magnetization relaxation time (τ) versus T^{-1} plot for **1** (○) and **2** (△) under zero DC field. The solid lines are the Arrhenius laws discussed in the text.

τ_0 significantly longer in **1** (×5.5), it is worth noting that the blocking temperatures are thus slightly higher in **1** than in **2** (at 1000 Hz, 4.3 and 3.7 K, respectively).

The relaxation times of these systems have been measured below 9 K, in other words in the regime of finite-size chain dynamics, where the following relation should be applied: $\Delta_\tau = \Delta_\xi + \Delta_A$ where Δ_A is the anisotropy energy gap.[2b,13] Considering the above estimations of Δ_τ ($\approx$ 55 K) and Δ_ξ ($\approx$ 34 K), an estimation of Δ_A for both systems is around 21 K that is about 2 K_A while it amounts K_A in the Ising limit. Therefore this result suggests that in these strongly correlated SCMs, the reversal of the spins involves collective flipping phenomenon that must be in relation with the presence of broad domain walls.

Conclusion

In summary, we have shown, by controlling both intra- and interchain magnetic interactions (J and J', respectively) in a $Mn^{III}Ni^{II}$ SCM system, that it is possible to make a magnet from an AF ordered phase of SCMs. In this remarkable AF phase, the slow dynamics is directly related to the intrinsic SCM properties of the isolated chains composing the material. Due to the similarity of the magnetic dynamics observed in both systems that display an AF ordered phase and a paramagnetic SCM ground state as exemplified by **1** and **2** described here, it is crucial to perform detailed static measurements to assign the "true" ground state of a system. It is very likely that some of the previously reported systems that have been described as SCMs have indeed an antiferromagnetic ground state. The results presented here and in reference [4] suggest that the simultaneous increase of both intra- and interchain magnetic interactions (with keeping $J \gg J'$), independently of the presence of an AF phase, is certainly an attractive research direction to design high temperature SCM-based magnets. This strategy can also be generalized to SMMs and thus, the introduction of large inter-SMM magnetic interactions could also lead to high temperature magnets based on SMM building blocks.

Experimental Section

Syntheses: All chemicals and solvents used during the syntheses were reagent grade. The Mn^{III} starting materials, $[Mn(3,5\text{-}Cl_2saltmen)(H_2O)(MeOH)]PF_6$ and $[Mn_2(5\text{-}Clsaltmen)_2(H_2O)_2](ClO_4)_2$ were synthesized by following the methods described elsewhere.[20,21] The Ni^{II} precursor, $[Ni(pao)_2(phen)]$, was prepared according to the literature method.[9]

$[Mn(3,5\text{-}Cl_2saltmen)Ni(pao)_2(phen)]PF_6$ (1): A solution of $[Ni(pao)_2(phen)]$ (194 mg, 0.25 mmol) in methanol/CH_2Cl_2 (10+5 mL) was added to a solution of $[Mn(3,5\text{-}Cl_2saltmen)(H_2O)(MeOH)]PF_6$ (173 mg, 0.127 mmol) in methanol (15 mL). After filtering the solution, the filtrate was kept undisturbed for several hours at room temperature to obtain gold-brown microcrystals of **1**. The products was collected by suction filtration, washed with methanol (10 mL), and dried in air. Large single crystals suitable for single-crystal X-ray crystallography could be obtained using a diffusion method of layered solutions of the precursors described above (upper layer: Mn solution; lower layer: Ni solution). The resulting crystals and the polycrystalline samples obtained from the bulk method are identical based on spectroscopic, magnetic, X-ray and elemental analyses. Note, that this diffusion method may give a contamination of a di-μ-oxo Mn^{IV} dinuclear species, $[\{Mn^{IV}(3,5\text{-}Cl_2saltmen)\}_2(\mu\text{-}O)_2]$. Therefore, the sample obtained by this method should be systematically checked by spectroscopic and analytical methods before magnetic measurements. For **1**·1.5 H_2O, bulk yield: 90%, 257 mg (0.22 mmol); elemental analysis calcd (%) for $C_{44}H_{39}N_8O_{5.5}F_6PCl_4MnNi$: C 45.24, H 3.36, N 9.59; found: C 45.34, H 3.41, N 9.57; IR (KBr): $\tilde{\nu}$ = 1601 (C=N), 559 (P–F), 843 (P–F) cm^{-1}.

$[Mn(5\text{-}Clsaltmen)Ni(pao)_2(phen)]BPh_4$ (2): This compound was synthesized by diffusing slowly two methanol solutions containing Mn^{III} and Ni^{II} starting materials, respectively. A solution of $[Mn_2(5\text{-}Clsaltmen)_2(H_2O)_2](ClO_4)_2$ (145 mg, 0.125 mmol) and $NaBPh_4$ (0.173 g, 0.51 mmol) in methanol (30 mL) and a solution (10 mL) of $[Ni(pao)_2(phen)]$ (205 mg, 0.25 mmol) were prepared and divided into portions, to fill up narrow diameter glass tubes (ø = 8 mm) for slow diffusion crystallization, where the lower and upper layers are the Ni^{II} and Mn^{III} solutions (1.4 and 4.3 mL), respectively. These glass tubes were kept undisturbed at room temperature until the diffusion was complete (about one week). Dark brown block-type crystals of **2** were collected by suction filtration, washed with methanol, and dried in air. For **2**·2.25 MeOH, Yield: 59% (193 mg, 0.15 mmol); elemental analysis calcd (%) for $C_{70.25}H_{67}BCl_2MnN_8NiO_{6.25}$: C 63.98, H 5.12, N 8.50; found: C 63.61, H 4.74, N 8.44; IR (KBr): $\tilde{\nu}$ = 1603 (C=N), 702 (B–C) cm^{-1}.

Physical characterizations: Infrared spectra were measured by using KBr disks with a Shimadzu FT-IR-8600 spectrophotometer. The magnetic susceptibility measurements were obtained with the use of a Quantum Design SQUID magnetometer MPMS-XL. This magnetometer works between 1.8 and 400 K for dc applied fields ranging from −7 to 7 T. The measurements were performed on finely grounded polycrystalline samples freshly prepared before measurements. ac susceptibility measurements have been measured with an oscillating ac field of 3 Oe and ac frequencies ranging from 1 to 1500 Hz. The magnetic data were corrected for the sample holder and the diamagnetic contributions. M vs H measurements have been performed at 100 K to check for the presence of ferromagnetic impurities that has been found systematically absent.

X-ray Crystallography: Single crystals of **1** and **2** were prepared by the method as described above. The single crystal for the crystallographic analysis was mounted on a glass rod. The crystal dimensions were 0.13 × 0.10 × 0.07 mm^3 for **1** and 0.52 × 0.22 × 0.18 mm^3 for **2**. Data collection was made on a Rigaku CCD diffractometer (Saturn 70) with graphite monochromated $Mo_{K\alpha}$ radiation (λ = 0.71069 Å) at a temperature of −180 ± 1 °C. The structures were initially solved by direct methods (SIR92 or SHELX97)[22] and expanded using Fourier techniques.[23] The non-hydrogen atoms were refined anisotropically, while hydrogen atoms were introduced as fixed contributors. It should be emphasized that the crystal of **1** had a non-merohedral twin, where twin component #1 composes 33.83% of the crystal. Full-matrix least-squares refinements on F^2 based on unique reflections were employed, where the unweighted and weighted agreement factors of $R = \Sigma||F_o| - |F_c||/\Sigma|F_o|$ ($I > 2.00\sigma(I)$), and $wR = [\Sigma w(F_o^2 - F_c^2)^2/\Sigma w(F_o^2)^2]^{1/2}$ were used. A Sheldrick weighting Scheme was used. All calculations were performed using the CrystalStructure software package of Molecular Structure Corporation.[24] CCDC 739107 (**1**) and 739108 (**2**) contain the supplementary crystallographic data for this paper. These data can be obtained free of charge from The Cambridge Crystallographic Data Centre via www.ccdc.cam.ac.uk/data_request/cif

Crystal data for **1**·CH_2Cl_2: $C_{45}H_{38}Cl_6F_6MnN_8NiO_4P$, M_r = 1226.17, triclinic, $P\bar{1}$, a = 10.314(2), b = 10.999(2), c = 22.348(5) Å, α = 87.043(17), β = 81.961(16), γ = 88.106(17)°, V = 2506.0(9) $Å^3$, T = 93(1) K, Z = 2, ρ_{calcd} = 1.625 $g\,cm^{-3}$, F_{000} = 1240.00, λ = 0.7107 Å, $\mu(Mo_{K\alpha})$ = 10.533 mm^{-1}, 21419 measured reflections, 9609 unique which were used in all calculations. R_1 = 0.0790 ($I > 2\sigma(I)$) and wR_2 = 0.1720 (all data) with GOF = 1.213.

Crystal data for **2**·2 CH_3OH: $C_{70}H_{66}BCl_2MnN_8NiO_6$, M_r = 1310.70, monoclinic, $P2_1/n$, a = 10.162(4), b = 19.405(7), c = 32.041(12) Å, β = 94.893(5)° V = 6295(4) $Å^3$, T = 93(1) K, Z = 4, ρ_{calcd} = 1.383 $g\,cm^{-3}$, F_{000} = 2728.00, λ = 0.7107 Å, $\mu(Mo_{K\alpha})$ = 6.448 mm^{-1}, 54201 measured reflections, 17180 unique which were used in all calculations. R_1 = 0.0695 ($I > 2\sigma(I)$) and wR_2 = 0.2079 (all data) with GOF = 1.002.

Acknowledgements

The authors acknowledge Dr. K. Sugimoto (RIGAKU Co. Ltd.) for his help in X-ray crystallography and Professor C. Coulon who teach us over the years the fascinating physics of this type of one-dimensional systems. This work was supported by the Sumitomo Foundation, a Grant-in-Aid for Scientific Research (No. 21655046) from the Ministry of Education, Culture, Sports, Science, and Technology, Japan, MAGMANet (NMP3-CT-2005-515767), the University of Bordeaux, the CNRS, the ANR (NT09_469563, AC-MAGnets project), GIS Advanced Materials in Aquitaine (COMET Project) and the Région Aquitaine.

[1] a) P. D. W. Boyd, Q. Li, J. B. Vincent, K. Folting, H.-R. Chang, W. E. Streib, J. C. Huffman, G. Christou, D. N. Hendrickson, *J. Am. Chem. Soc.* **1988**, *110*, 8537; b) A. Caneschi, D. Gatteschi, R. Sessoli, *J. Am. Chem. Soc.* **1991**, *113*, 5873; c) R. Sessoli, H.-L. Tsai, A. R. Schake, S. Wang, J. B. Vincent, K. Folting, D. Gatteschi, G. Christou, D. N. Hendrickson, *J. Am. Chem. Soc.* **1993**, *115*, 1804; d) D. Gatteschi, R. Sessoli, J. Villain, *Molecular Nanomagnets*, Oxford University Press, Oxford, **2006**.

[2] a) R. Clérac, H. Miyasaka, M. Yamashita, C. Coulon, *J. Am. Chem. Soc.* **2002**, *124*, 12837; b) C. Coulon, H. Miyasaka, R. Clérac, *Struct. Bonding (Berlin)* **2006**, *122*, 163.

[3] A. Caneschi, D. Gatteschi, N. Lalioti, C. Sangregorio, R. Sessoli, G. Venturi, A. Vindigni, A. Rettori, M. G. Pini, M. A. Novak, *Angew. Chem.* **2001**, *113*, 1810; *Angew. Chem. Int. Ed.* **2001**, *40*, 1760.

[4] C. Coulon, R. Clérac, W. Wernsdorfer, T. Colin, H. Miyasaka, *Phys. Rev. Lett.* **2009**, *102*, 167204/1–4.

[5] N. Ishii, Y. Okamura, S. Chiba, T. Nogami, T. Ishida, *J. Am. Chem. Soc.* **2008**, *130*, 24; T. Ishida, Y. Okamura, I. Watanabe, *Inorg. Chem.* **2009**, *48*, 7012.

[6] R. Sessoli, *Angew. Chem.* **2008**, *120*, 5590; *Angew. Chem. Int. Ed.* **2008**, *47*, 5508.

[7] H. Miyasaka, A. Saitoh, S. Abe, *Coord. Chem. Rev.* **2007**, *251*, 2622.

[8] H. Miyasaka, R. Clérac, *Bull. Chem. Soc. Jpn.* **2005**, *78*, 1725.

[9] a) H. Miyasaka, K. Mizushima, K. Sugiura, M. Yamashita, *Synth. Met.* **2003**, *137*, 1245; b) H. Miyasaka, S. Furukawa, S. Yanagida, K. Sugiura, M. Yamashita, *Inorg. Chim. Acta* **2004**, *357*, 1619; c) H. Miyasaka, A. Saitoh, S. Yanagida, C. Kachi-Terajima, K. Sugiura, M. Yamashita, *Inorg. Chim. Acta* **2005**, *358*, 3525.

[10] M. Ferbinteanu, H. Miyasaka, W. Wernsdorfer, K. Nakata, K. Sugiura, M. Yamashita, C. Coulon, R. Clérac, *J. Am. Chem. Soc.* **2005**, *127*, 3090.

[11] a) H. Miyasaka, R. Clérac, K. Mizushima, K. Sugiura, M. Yamashita, W. Wernsdorfer, C. Coulon, *Inorg. Chem.* **2003**, *42*, 8203; b) A. Saitoh, H. Miyasaka, M. Yamashita, R. Clérac, *J. Mater. Chem.*

2007, *17*, 2002; c) H. Miyasaka, A. Saitoh, M. Yamashita, R. Clérac, *Dalton Trans.* **2008**, 2422.
[12] H. Miyasaka, M. Julve, M. Yamashita, R. Clérac, *Inorg. Chem.* **2009**, *48*, 3420.
[13] C. Coulon, R. Clérac, L. Lecren, W. Wernsdorfer, H. Miyasaka, *Phys. Rev. B* **2004**, *69*, 132408; W. Wernsdorfer, R. Clérac, C. Coulon, L. Lecren, H. Miyasaka, *Phys. Rev. Lett.* **2005**, *95*, 237203; C. Coulon, R. Clérac, W. Wernsdorfer, T. Colin, A. Saitoh, N. Motokawa, H. Miyasaka, *Phys. Rev. B* **2007**, *76*, 214422.
[14] M. Drillon, E. Coronado, D. Beltran, R. Georges, *Chem. Phys.* **1983**, *79*, 449; R. Georges, J. J. Borras-Almenar, E. Coronado, J. Curely, M. Drillon, *Magnetism: Molecules to Materials I: Models and Experiments* (Eds.: J. S. Miller, M. Drillon), Wiley-VCH, Weinheim, **2002**, p. 1.
[15] J. M. Loveluck, S. W. Lovesey, S. Aubry, *J. Phys. C* **1975**, *8*, 3841.
[16] K. Nakamura, T. Sasada, *J. Phys. C* **1978**, *11*, 331.
[17] K. Nakamura, T. Sasada, *Solid State Commun.* **1977**, *21*, 891.
[18] B. Barbara, *J. Physique* **1973**, *34*, 1034; B. Barbara, *J. Magn. Magn. Mater.* **1994**, *129*, 79.
[19] To link H_a to the anisotropy energy, K_A, a phenomenological approach considering a chain of classical spins can be used at low temperature when the exchange energy is much larger than any other energy scale of the system. In this limit, the magnetization (M) when the field is applied perpendicularly to the easy axis is obtained by minimizing the effective energy: $E_{eff} = K_A\sin^2(\theta) - \mu_B H(g_{Mn}S_{Mn} - g_{Ni}S_{Ni})\sin(\theta)$ (θ is the angle between the effective spins and the easy axis). The resulting M at equilibrium is $M=(g_{Mn}S_{Mn}-g_{Ni}S_{Ni})\mu_B\sin(\theta_{min})$ deduced from the minimization of E_{eff} by simple derivation: $dE_{eff}/d\theta=0$. The magnetization saturation is obtained for $\sin(\theta_{min})=1$ leading to $2K_A=(g_{Mn}S_{Mn}-g_{Ni}S_{Ni})\mu_B H_a$.
[20] H. Miyasaka, R. Clérac, T. Ishii, H.-C. Chang, S. Kitagawa, M. Yamashita, *J. Chem. Soc. Dalton Trans.* **2002**, 1528.
[21] H. Miyasaka, T. Nezu, K. Sugimoto, K. Sugiura, M. Yamashita, R. Clérac, *Chem. Eur. J.* **2005**, *11*, 1592.
[22] a) SIR92: A. Altomare, M. C. Burla, M. Camalli, M. Cascarano, C. Giacovazzo, A. Guagliardi, G. Polidori, *J. Appl. Crystallogr.* **1994**, *27*, 435 b) SHELX97, G. M. Sheldrick, **1997**.
[23] DIRDIF94, P. T. Beurskens, G. Admiraal, G. Beurskens, W. P. Bosman, R. de Gelder, R. Israel, J. M. M. Smits, **1994**.
[24] CrystalStructure 3.8, Crystal Structure Analysis Package, Rigaku and Rigaku Americas, 9009 New Trails, The Woodlands, TX 77381, **2000–2007**.

Received: October 16, 2009
Published online: February 11, 2010

